AAC Journals.ASM.org

Combined Spatial Limitation around Residues 16 and 108 of *Plasmodium falciparum* Dihydrofolate Reductase Explains Resistance to Cycloguanil

Jarunee Vanichtananukul,[a] Supannee Taweechai,[a] Chayasith Uttamapinant,[a] Penchit Chitnumsub,[a] Tirayut Vilaivan,[b] Yongyuth Yuthavong,[a] and Sumalee Kamchonwongpaisan[a]

National Centre for Genetic Engineering and Biotechnology, National Science and Technology Development Agency, Klong Luang, Pathumthani, Thailand,[a] and Department of Chemistry, Faculty of Science, Chulalongkorn University, Patumwan, Bangkok, Thailand[b]

Natural mutations of *Plasmodium falciparum* dihydrofolate reductase (*Pf*DHFR) at A16V and S108T specifically confer resistance to cycloguanil (CYC) but not to pyrimethamine (PYR). In order to understand the nature of CYC resistance, the effects of various mutations at A16 on substrate and inhibitor binding were examined. Three series of mutations at A16 with or without the S108T/N mutation were generated. Only three mutants with small side chains at residue 16 (G, C, and S) were viable from bacterial complementation assay in the S108 series, whereas these three and an additional four mutants (T, V, M, and I) with slightly larger side chains were viable with simultaneous S108T mutation. Among these combinations, the A16V+S108T mutant was the most CYC resistant, and all of the S108T series ranged from being highly to moderately sensitive to PYR. In the S108N series, a strict requirement for alanine was observed at position 16. Crystal structure analyses reveal that in *Pf*DHFR-TS variant T9/94 (A16V+S108T) complexed with CYC, the ligand has substantial steric conflicts with the side chains of both A16V and S108T, whereas in the complex with PYR, the ligand only showed mild conflict with S108T. CYC analogs designed to avoid such conflicts improved the binding affinity of the mutant enzymes. These results show that there is greater spatial limitation around the S108T/N residue when combined with the limitation imposed by A16V. The limitation of mutation of this series provides opportunities for drug design and development against antifolate-resistant malaria.

Plasmodium falciparum dihydrofolate reductase (*Pf*DHFR) is one of the most well-defined drug targets in malaria chemotherapy with such antifolates as pyrimethamine (PYR) and cycloguanil (CYC; administered as proguanil) among its inhibitors (26). It catalyzes the NADPH-dependent reduction of 7,8-dihydrofolate (DHF) to 5,6,7,8-tetrahydrofolate (THF) in the biosynthesis of deoxythymidylate (dTMP). After decades of antifolate deployment, the parasite has become increasingly resistant to PYR and CYC due to mutations that reduce the binding affinity of inhibitors. While *Pf*DHFR mutations at residues 108, 59, 51, and 164 confer cross-resistance to both PYR and CYC, the double-mutation variant A16V+S108T specifically confers resistance to CYC. The CYC-resistant mutant was postulated to have arisen by the S108T mutation followed by A16V, giving rise to high CYC resistance without a loss in catalytic efficiency (18). Molecular modeling suggests that the A16V mutation causes steric clash between the side chain and one of the 2,2-dimethyl groups of CYC (15). PYR, on the other hand, avoids such a steric clash, presumably due to lack of a group equivalent to the methyl of CYC (15). However, the lack of crystal structure data for the A16V+S108T *Pf*DHFR and its complex with CYC makes such conclusion a tentative one.

Unlike cumulative mutations in the S108N series of PYR resistance-generating mutant *Pf*DHFRs, no other resistant variants in the S108T series apart from A16V+S108T have been identified from the field. Laboratory selection for PYR resistance in a wild-type parasite strain led to the identification of mutants with a single mutation at either A16S or I164M (22). In the same study, selection for increased PYR resistance in the *Pf*DHFR-TS A16V+S108T mutant strain T9/94 demonstrated DHFR-TS gene amplification but no further mutation of the protein (22). Another study of laboratory-induced PYR resistance reported A16V+S108T variants with additional mutations at F223S and D54N (20). The A16V+S108T+D54E+F223S mutant enzyme shows enhanced resistance to CYC and is also resistant to PYR (19).

We investigated here the effect of mutation at residue 16 on *Pf*DHFR catalytic activity and antifolate resistance. In the presence or the absence of the S108T/N mutation, mutants of A16X were catalytically active only when X was an amino acid with a small side chain, suggesting limitation in space around residue 16. Crystal structures of *Pf*DHFR-TS T9/94 variant (A16V+S108T) in complex with CYC and PYR were determined to reveal the different modes of inhibitor binding. The structural information presented here shows confinement of the DHFR binding pocket at subsites containing residues 16 and 108, with the mutual effects of steric constraint in one subsite exerting further confinement on another subsite. Such mutual effects are present in the binding of CYC, which has a 2-methyl group in conflict with the side chain of V16, and a *p*-chlorine atom in conflict with the side chain of T108. These constraints are absent in the binding of PYR, which lacks an equivalent group in the vicinity of V16. Therefore, the resistance

Received 9 February 2012 Returned for modification 26 March 2012
Accepted 16 April 2012
Published ahead of print 23 April 2012
Address correspondence to Sumalee Kamchonwongpaisan, sumaleek@biotec.or.th.

doi:10.1128/AAC.00301-12

of the A16V+S108T *Pf*DHFR-bearing parasite only to CYC, but not to PYR, is explained. This information should help in the design of effective inhibitors against mutant *Pf*DHFRs and against antifolate-resistant malaria.

MATERIALS AND METHODS

Construction of mutant libraries. Mutant libraries of A16-saturated mutations were generated by QuikChange site-directed mutagenesis using pET17b containing synthetic *Pf*DHFR–A16V+S108T gene as a template, 5′-C TTT GAC ATC TAC GCT ATC TGC [NNG/C] TGC TGT AAA GTT GAA AGC AAA-3′ as the sense primer, and 5′-TTT GCT TTC AAC TTT ACA GCA [G/CNN] GCA GAT AGC GTA GAT GTC AAA G-3′ as the antisense primer, where the A16X codon is marked by brackets, and N represents all four bases. The mutagenesis reaction contained 40 ng of template, 125 ng of each primer, 1× *Pfu* buffer, and 10 U of *Pfu* DNA polymerase (Promega) and was carried out using the following temperature cycling profile: 95°C for 5 min, followed by 20 cycles of 95°C for 30 s, 45°C for 1 min, and 68°C for 8 min, with a final incubation at 68°C for 10 min. The mutagenesis product was digested with 20 U of DpnI at 37°C for 1 h and then transformed into *E. coli* DH5α. Recombinant clones grown on Luria-Bertani (LB) agar with 100 μg of ampicillin (Amp) ml^{-1} were randomly selected for sequencing. Generation of A16X+S108 series was performed using the same protocol with an equimolar mixture of the 20 identified A16X+S108T as templates and a pair of primers that allowed mutation of T108 back to S108—5′-GTT GTT ATG GGC CGC ACC TCG TGG GAA TCG ATT CCG AAA AAA TTC-3′ and 5′-GAA TTT TTT CGG AAT CGA TTC CCA CGA GGT GCG GCC CAT AAC AAC-3′—as the sense and antisense primers, respectively. A16X mutants in the N108 series were limited to G, C, S, T, and V. The mutagenesis reactions were performed separately using specific templates from the T108 series and a pair of primers that allowed the mutation of T108N: 5′-GGG CCG CAC CAA CTG GGA ATC GAT-3′ and 5′-ATC GAT TCC CAG TTG GTG CGG CCC-3′. The clones obtained were verified by automated Sanger sequencing to ensure that there were no adventitious mutations in the course of making the site-specific mutations.

Screening of active DHFR mutants by bacterial complementation assay. Plasmids from the pET-*Pf*DHFR mutants were retransformed into *E. coli* BL21(DE3)/pLysS. The transformants were grown on LB agar with 100 μg of Amp ml^{-1} and 34 μg of chloramphenicol (Cam) ml^{-1}. The mutant clones were screened for *Pf*DHFR activity by streaking them on minimal medium containing 100 μg of Amp ml^{-1} and 34 μg of Cam ml^{-1} with or without 4 μM trimethoprim. After overnight incubation at 37°C, transformed bacteria are only able to grow in the presence of trimethoprim if the *Pf*DHFR has adequate activity; mutants with low activity do not support growth (4).

Expression and purification of mutant *Pf*DHFRs. All of the mutants were expressed in *E. coli* BL21(DE3)/pLysS by cultivation in LB supplemented with 100 μg of Amp ml^{-1} and 34 μg of Cam ml^{-1} and 0.4 mM IPTG (isopropyl-β-D-thiogalactopyranoside) induction at 20°C for 24 h. The expression levels of all mutants were confirmed by SDS-PAGE. The relative *Pf*DHFR activity of each mutant compared to wild-type enzyme was determined from crude protein extracts. Those with relative crude activity higher than 3% were further purified by methotrexate-Sepharose affinity chromatography (17) and anion exchange as previously described (2, 9).

Enzyme kinetic analysis and inhibition by antifolates. DHFR activities were determined spectrophotometrically using a Hewlett Packard UV-VIS spectrophotometer (HP8453) in a 1-ml reaction containing 100 μM concentrations each of dihydrofolate and NADPH in 50 mM TES (pH 7.0), 75 mM β-mercaptoethanol, 1 mg of bovine serum albumin ml^{-1}, and the appropriate amount of purified enzyme (1 to 5 mU) to initiate the reaction. PYR, CYC, WR99210, and a series of CYC analogues (15, 27) were 2-fold serial diluted in dimethyl sulfoxide in 96-well plates (200 μl, final well volume), and binding constants were determined using the protocol described previously (21). Kinetic parameters were calculated by a nonlinear least-square fit of the data to the Michaelis-Menten equation using the software Kaleidagraph 3.51 as previously described (9, 21).

Crystallization, data collection, and structure determination. The bifunctional DHFR-TS enzymes of both wild-type strain TM4 and the A16V+S108T mutant strain T9/94 of *P. falciparum* were cloned, expressed, and purified as previously described (2, 28). Protein was cocrystallized with either 2 mM CYC or 2 mM PYR in the presence of NADPH and dUMP. X-ray diffraction data were collected at the CuKα wavelength (1.5418 Å) on a Bruker-Nonius FR591 X-ray generator equipped with a κCCD detector. The data were indexed, integrated and scaled using the Denzo/Scalepack program in the HKL-2000 package (14). The data were directly refined at 3.0-Å resolution using *Pf*DHFR-TS TM4 (PDB 1J3I) as a template in the Crystallography and NMR System (1, 28). The models were iteratively rebuilt and adjusted in program *O* (8) and gradually refined to the highest resolution in CNS (1). Ligands and water molecules were added to a positive Fourier difference electron density map ($F_o - F_c$). The final models were verified by PROCHECK (11) with Ramachandran parameters listed in Table 1. Structural figures were prepared with PyMOL (16).

PDB accession codes. Coordinates and structure factors have been deposited in the Protein Data Bank (PDB) under accession codes 3UM5, 3UM6, and 3UM8.

RESULTS

Screening of active A16X+S108T/N *Pf*DHFR mutants. Constructs of wild-type and 45 A16X mutants with S108 or S108N/T mutations were successfully generated and verified by DNA sequencing. These mutants included 19 from the A16X+S108 series, 20 from the A16X+S108T series, and 6 from the S108N series. For the S108N series, only the A16 mutants that are capable of complementing bacterial growth in the S108T series were created, i.e., G, A, C, S, T, and V.

The activities of the wild-type and mutant *Pf*DHFRs in *E. coli* BL21(DE3)/pLysS were screened by complementation assay. Only six mutants from S108T series showed adequate activity for growth, namely, S108T, A16C+S108T, A16G+S108T, A16S+S108T, A16T+S108T, and A16V+S108T. Hence, only the amino acids with small side chains at position 16 when combined with S108T were functionally active. Moreover, two mutants with slightly larger side chains at position 16, namely, A16I+S108T and A16M+S108T, could also complement host DHFR under the same conditions, albeit poorly (Table 2). Further investigation of the S108 series showed that only the wild type and three mutants (A16G, A16S, and A16C) were found to be catalytically active by bacterial complementation assay, while the others were not. In the S108N series, only alanine was tolerated at position 16 among the six mutants tested.

Crude extracts of wild-type *Pf*DHFR and 45 mutants with A16X and S108 or S108N/T were prepared in 50 ml of LB broth with IPTG induction in order to examine their expression levels and DHFR activities. SDS-PAGE analysis of the crude extracts revealed that all of the constructs expressed *Pf*DHFR similarly to the wild-type construct (data not shown). However, these crude extracts exhibited a wide range of enzyme specific activities. The relative DHFR activity of crude protein extracts of the active mutants, defined from the ability to complement bacterial DHFR in the presence of trimethoprim in bacterial complementation assay, ranged from 1.4 to 62.4% of the wild-type enzyme (Table 3), while the activities of the inactive mutants were negligible. The results are in line with our previous reports, wherein only constructs expressing relative DHFR activity higher than 1.3% of the wild-

TABLE 1 Data collection and refinement statistics of crystal structures

Parameter[a]	Enzyme and ligand		
	*Pf*DHFR-TS T9/94		
	PYR	CYC	*Pf*DHFR-TS TM4 (CYC)
Data collection			
Space group	$P2_12_12_1$	$P2_12_12_1$	$P2_12_12_1$
Unit cell parameters (Å)			
a	56.529	56.696	58.761
b	155.119	155.549	157.538
c	165.257	164.962	164.509
Resolution* (Å)	30–2.40 (2.49–2.40)	30–2.65 (2.74–2.65)	50–2.60 (2.69–2.60)
R_{merge}* (%)	6.5 (35.1)	7.9 (35.5)	4.1 (25.8)
$I/\sigma I$*	15.5 (3.0)	19.2 (4.2)	20.3 (4.3)
Completeness* (%)	98.7 (95.0)	99.9 (99.7)	98.4 (93.2)
Redundancy	4.6	8.1	4.4
Refinement			
Resolution (Å)	30–2.40	30–2.65	50–2.60
No. reflections (unique)	56,048	43,280	47,165
R_{work}/R_{free}[b]	20.2/25.4	20.3/25.7	21.2/25.8
No. of atoms			
Protein	9,058	9,048	9,046
PYR or CYC	34	34	34
NADPH	96	96	96
dUMP	40	40	
Water	781	371	456
Phosphate			10
Avg B factor (Å^2)	46.9	48.5	52.5
Ramachandran plot (%)			
Favored region	85.6	84.6	87.3
Additional allowed region	14.2	15.2	12.3
Generously allowed region	0.2	0.2	0.2
Disallowed region	0	0	0.2[c]
RMS deviations			
Bond length (Å)	0.006	0.007	0.008
Bond angle (°)	1.4	1.4	1.5

[a] *, Values in parentheses are for the highest-resolution shell. RMS, root mean square.
[b] R_{free} is calculated from 5% of reflections chosen randomly in each of the 10 resolution bins.
[c] Lys49 is located on a flexible loop of each molecule of *Pf*DHFR-TS.

type enzymes could support bacterial growth on trimethoprim plates (4, 9).

Kinetic parameters of *Pf*DHFR mutants. Wild-type *Pf*DHFR and 10 active A16X *Pf*DHFR mutants with or without S108T/N mutations were purified to homogeneity and enzyme kinetic parameters determined. As summarized in Table 3, the k_{cat} values of all of the active mutants varied from 1.6 to 86% of that of the wild-type enzyme. Among these mutants, A16C+S108T exhibited the highest k_{cat} value, while A16T+S108T was the lowest. The k_{cat} values of the others were 14 to 51% of the wild-type enzyme.

Mutations of A16 and S108 affected DHF binding to various degrees. The A16S and S108N mutants showed 3- to 4-fold-higher K_m values for DHF than those of the wild type, while the K_m values for the S108T and A16C+S108T mutants were about 2- to 4-fold less. Unlike DHF, the K_m values for NADPH were not much affected by mutations since the values were within a 2-fold range of the wild-type enzyme. Among the 10 active mutants, A16C+S108T and S108T showed the highest catalytic efficiency (k_{cat}/K_m), about 1.4- to 1.6-fold that of the wild-type enzyme. The catalytic efficiency of the other mutants, including A16V+S108T, was about 4 to 38% that of the wild-type enzyme and that of A16T+S108T was <1%.

Antifolate sensitivity of *Pf*DHFR mutants. The inhibition constants (K_i) of PYR, CYC, and WR99210, as well as of three CYC derivatives, namely, C17 (R^1, R^2, and R^3 = H, Me, and *p*-Cl phenyl, respectively), C88 (R^1, R^2, and R^3 = Me, Me, and *m*-Cl phenyl, respectively), and C248 (R^1, R^2, and R^3 = H, Me, and *m*-Cl phenyl, respectively), against the 10 mutants were determined in order to understand the drug resistance pattern of the active mutants. The data are summarized in Table 4.

Among the three active A16X single mutants, only A16S was highly resistant to CYC, with K_i values ~83 times higher than that of the wild type, while the others were about 1- to 3.5 times that of the wild type. In combination with S108T mutation, the K_i values of CYC against all of the active double mutants were markedly increased, i.e., by about 58- to 1,014-fold that of the wild-type and 20- to 345-fold that of the S108T single mutant. In addition, the K_i values of CYC against S108N were 8 times that of the wild-type enzyme and 2.7 times that of S108T. These results suggested that the steric conflicts of the *p*-Cl group at R^3 and a 2-methyl group of

TABLE 2 Summary of bacterial complementation assay of *Pf*DHFR activities in *E. coli* BL21(DE3)/pLysS on a minimal medium plate in the presence of trimethoprim[a]

Amino acid at residue 16	Type	Residue vol[b] (Å^3)	Surface area[c] (Å^2)	Bacterial complementation		
				S108	T108	N108
G	Aliphatic	60.1	75	+	+	–
A (wild type)	Aliphatic	88.6	115	+	+	+
P	Aliphatic	112.7	145	–	–	NA[d]
V	Aliphatic	140.0	155	–	+	–
M	Aliphatic	162.9	185	–	+/–	NA
I	Aliphatic	166.7	175	–	+/–	NA
L	Aliphatic	166.7	170	–	–	NA
S	Polar, uncharged	89.0	115	+	+	–
C	Polar, uncharged	108.5	135	+	+	–
N	Polar, uncharged	114.1	160	–	–	NA
T	Polar, uncharged	116.1	140	–	+	–
Q	Polar, uncharged	143.8	180	–	–	NA
H	Positively charged	153.2	195	–	–	NA
K	Positively charged	168.6	200	–	–	NA
R	Positively charged	173.4	225	–	–	NA
D	Negatively charged	111.1	150	–	–	NA
E	Negatively charged	138.4	190	–	–	NA
F	Aromatic	189.9	210	–	–	NA
Y	Aromatic	193.6	230	–	–	NA
W	Aromatic	227.8	255	–	–	NA

[a] The results are indicated as positive (+) and negative (–) for bacterial growth and no growth, respectively.
[b] Zamyatnin (29).
[c] Chothia (3).
[d] NA, not analyzed.

CYC with side chains of amino acid residues 108 and 16, respectively, are significant and that the clash with S108N exerted a greater effect on the binding affinity than that of S108T, which is in line with previous observations (18).

In order to reduce the steric clash of inhibitors with A16X mutants, the inhibitor C17 was designed with only one methyl group at the position 2 of the dihydrotriazine ring (either R^1 or R^2), while maintaining its *p*-Cl phenyl group at R^3. The K_i values of C17 against the wild type and most of mutants were generally similar to those of CYC (0.2- to 2.2-fold) but reduced markedly by 10.7-fold against A16V+S108T compared to CYC. By moving the *p*-Cl group to the *m*-position to avoid steric clash with S108T while preserving the 2,2-dimethyl groups of CYC, the inhibitor C88 showed reduction of K_i values against all of the double mutants to an even greater extent than C17, by 4- to 41-fold compared to CYC. With the combination of both features so as to avoid steric conflicts on both sites, C248 (desmethyl and *m*-Cl phenyl) showed dramatically lower K_i values against A16V+S108T by a factor of 51 compared to that of CYC (from 1,518 nM for CYC to 30 nM for C248). The K_i values against other

TABLE 3 Crude enzyme activity and kinetic properties of purified *Pf*DHFR wild-type and mutant enzymes of A16X with or without the S108 T/N mutation

Enzyme	Crude enzyme activity		Kinetic parameters of purified enzyme[a]			
	Mean sp act (nmol/min/mg) ± SD	Relative activity	Mean K_m ± SD (μM)		k_{cat} (s^{-1})	k_{cat}/K_m
			DHF	NADPH		
Wild type (A16+S108)	1,978 ± 284	100	12.2 ± 2.0	5.8 ± 1.7	72.9	5.9
S108N	516 ± 147	26.1	32.5 ± 1.8	3.7 ± 0.4	36.1	1.1
S108T	1,235 ± 232	62.4	3.0 ± 0.6	2.1 ± 0.6	24.7	8.2
A16C	274 ± 33	13.8	16.4 ± 1.7	3.6 ± 0.6	37.4	2.3
A16G	77 ± 21	3.9	15.2 ± 2.3	11.7 ± 2.0	10.4	0.68
A16S	130 ± 5	6.6	47.6 ± 1.1	4.8 ± 0.3	10.8	0.23
A16C+S108T	1,181 ± 198	59.7	6.6 ± 0.6	4.7 ± 1.3	62.6	9.5
A16G+S108T	176 ± 33	8.9	10.2 ± 1.5	7.9 ± 1.4	16.9	1.7
A16S+S108T	733 ± 195	37.1	19.4 ± 3.3	2.4 ± 0.3	16.6	0.86
A16T+S108T	70 ± 7	3.5	23.8 ± 1.8	2.3 ± 0.1	1.2	0.05
A16V+S108T	241 ± 49	12.2	21.3 ± 2.9	4.5 ± 0.5	18.9	0.89
A16M+S108T	33 ± 7	1.7	ND	ND	ND	ND
A16I+S108T	27 ± 2	1.4	ND	ND	ND	ND

[a] ND, not determined.

TABLE 4 Inhibition constant (K_i) of *Pf*DHFR wild-type and mutant enzymes of A16X combination with or without the S108T/N mutation

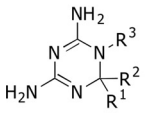

Inhibitor	R^1	R^2	R^3
CYC	CH_3	CH_3	p-ClC_6H_4
C17	H	CH_3	p-ClC_6H_4
C88	CH_3	CH_3	m-ClC_6H_4
C248	H	CH_3	m-ClC_6H_4
WR99210	CH_3	CH_3	2,4,5-$Cl_3C_6H_2O(CH_2)_3O$

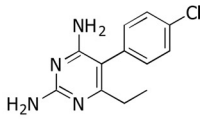

PYR

	Mean K_i ± SD (nM)					
Enzyme	CYC	C17	C88	C248	WR99210	PYR
Wild type	1.6 ± 0.3	3.9 ± 0.5	3.0 ± 0.1	6.0 ± 0.2	0.4 ± 0.2	0.6 ± 0.1
S108N	13 ± 0.4	53 ± 6.0	2.8 ± 0.5	8.8 ± 1.8	1.1 ± 0.1	14 ± 2.1
S108T	4.7 ± 0.8	25 ± 2.9	8.1 ± 1.5	5.2 ± 0.8	0.1 ± 0.03	0.6 ± 0.07
A16C	1.8 ± 0.2	6.1 ± 0.4	6.3 ± 0.3	5.0 ± 0.4	0.8 ± 0.1	0.8 ± 0.1
A16G	5.5 ± 0.9	43 ± 12	16 ± 3.8	53 ± 10	1.1 ± 0.1	1.4 ± 0.3
A16S	132 ± 23	497 ± 78	259 ± 45	780 ± 90	4.6 ± 0.5	12 ± 1.1
A16C+S108T	93 ± 15	42 ± 4	7.6 ± 1.1	7.9 ± 1.3	0.1 ± 0.02	0.3 ± 0.1
A16G+S108T	135 ± 28	250 ± 34	16 ± 1.0	46 ± 0.6	0.2 ± 0.05	0.7 ± 0.05
A16S+S108T	733 ± 126	711 ± 64	18 ± 2.5	94 ± 12	0.4 ± 0.05	0.7 ± 0.1
A16T+S108T	1,623 ± 199	1,809 ± 212	369 ± 25	344 ± 22	0.6 ± 0.03	0.9 ± 0.1
A16V+S108T	1,518 ± 503	142 ± 8	330 ± 61	30 ± 2	0.7 ± 0.1	0.6 ± 0.2

A16X+S108T mutants were also reduced by factors of 3 to 12 compared to CYC. Unlike CYC and its derivatives, PYR with *p*-Cl phenyl at R^3 remained effective against most of the mutants created. The K_i values of PYR against the active mutants were mostly <1 nM. Only the A16S and S108N mutants showed slightly poorer binding to PYR, with K_i values of 12 and 14 nM, respectively, mainly due to their high DHF K_m value. Likewise, WR99210, a flexible antifolate, also remained effective against the entire collection of active *Pf*DHFR mutants. The WR99210 K_i values against these mutants ranged from 0.1 to 1.1 nM, with the highest K_i value of 4.6 nM against the A16S mutant.

Structure analysis of *Pf*DHFR-TS from T9/94 strain. Four crystal structures of the *Pf*DHFR-TS wild type (TM4, PYR/CYC sensitive) and A16V+S108T (T9/94, PYR sensitive and CYC resistant) in complex with PYR (TM4-PYR [PDB 3QGT] and T9/94-PYR) and CYC (TM4-CYC and T9/94-CYC) were studied in order to understand the basis of A16V+S108T resistance to CYC. Superimposition of TM4-CYC to TM4-PYR (Fig. 1A) showed similar overall structures, with only a slight shift of CYC, as indicated by movement of the *p*-Cl group of CYC 0.8 Å away from that of PYR in TM4-PYR. The fact that TM4 is sensitive to CYC (K_i value of 1.6 nM, Table 4) suggests that the slight shift does not affect the binding affinity of CYC in the TM4 variant. Similarly, the superposition of T9/94-PYR to TM4-PYR (Fig. 1B) also revealed an unchanged overall structure of the DHFR enzyme active site and only a minor displacement of PYR due to a slight clash of the γ-CH_3 group of T108 of T9/94 with the *p*-Cl group of PYR. This is seen from a shift of the *p*-Cl group of PYR in T9/94-PYR by 0.8 Å and a slight twist of the phenyl ring of PYR in T9/94-PYR by 6.8° (the torsion angle of the two rings of PYR changed from 111.1° to 104.3° in TM4-PYR and T9/94-PYR, respectively). The displacement of PYR in the T9/94 binding pocket is an adjustment, which does not have any significant effect on the PYR binding affinity, since the T9/94 remains sensitive to PYR (K_i value = 0.6 nM for both, Table 4).

In contrast, in the structure of T9/94-CYC superposed on TM4-CYC (Fig. 1C), a slightly outward shift of the backbone of the T9/94 around V16 and T108 to expand the active site chamber was observed, presumably due to restricted space. Furthermore, the β-branched side chains of S108T and A16V in T9/94-CYC cause steric conflict to the *p*-Cl group and one of the 2,2-dimethyl groups of CYC, respectively, and hence the displacement of CYC molecule in T9/94-CYC, as evidenced from a 1.3-Å shift of the *p*-Cl group and a 0.8-Å shift of 2,2-dimethyl groups compared to CYC in the TM4-CYC structure. The *p*-Cl phenyl ring of CYC is twisted by 10.6° (the torsion angles of the two rings of CYC changed from 108.9° to 98.3° in TM4-CYC and T9/94-CYC, respectively). Superposition of T9/94-CYC to T9/94-PYR (Fig. 1D) clearly confirms that the steric conflict is much more pronounced on CYC than on PYR, as shown by the movement of the side chain of V16 of the T9/94-CYC by 0.4 Å compared to that of T9/94-PYR. The conflict also resulted in a shift of the *p*-Cl group of CYC by 1.6 Å compared to T9/94-PYR. This would explain the very high K_i value of T9/94-CYC (K_i value = 1,518 nM, Table 4). The higher degree of displacement of CYC in T9/94-CYC, compared to PYR in T9/94-PYR, suggested a less favorable binding interaction with the enzyme, thus causing CYC resistance in the T9/94 strain.

Taken altogether, these results indicated that the steric hindrance caused by A16V and S108T in the active site of T9/94-CYC aggravate the binding of CYC, but not PYR. This is reflected by the poor binding affinity of CYC to A16V+S108T, which results in resistance of T9/94 parasite to CYC, but not to PYR.

DISCUSSION

It has been well established that mutations of *Pf*DHFR are responsible for antifolate resistance in *P. falciparum*. *Pf*DHFR mutants in the S108N series are resistant to both CYC and PYR, while A16V+S108T, the only member of the S108T series, confers resistance to CYC only. In this report, we confirm that the mutation of residue A16 to V16 in the presence of S108T is indeed the outcome of a compromise between its catalytic activity and CYC resistance.

In combination with or without S108T/N mutation, only 12 mutants of A16X enzymes were catalytically active, as revealed by

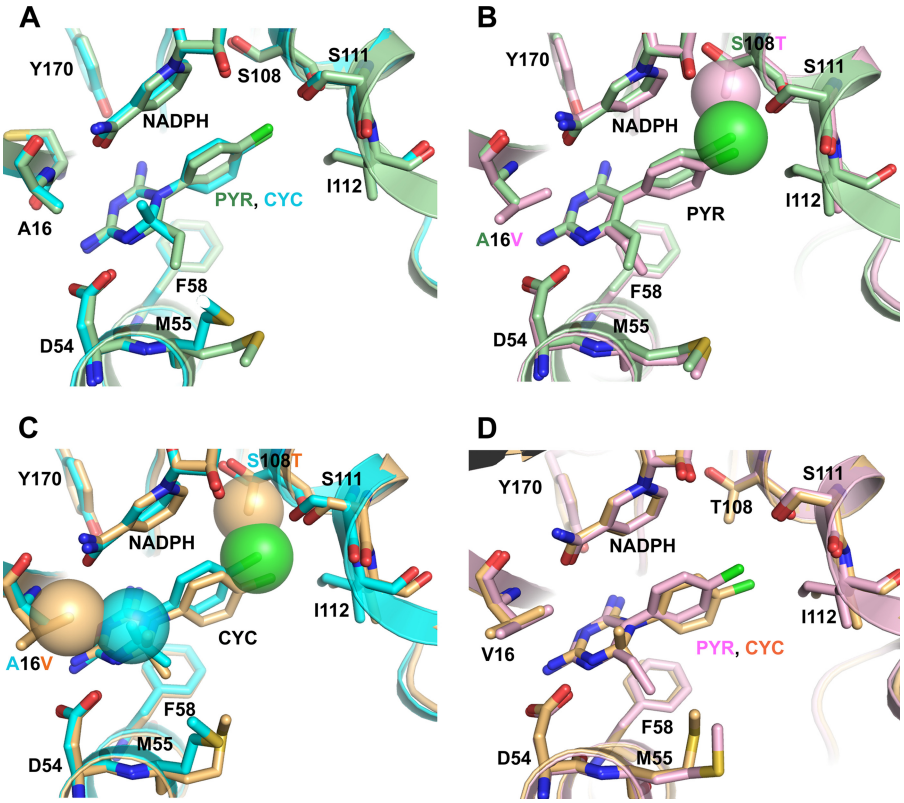

FIG 1 Comparison of cocrystal structures of *Pf*DHFR domains with CYC and PYR. (A) Superposition of the wild-type *Pf*DHFR in complex with PYR (TM4-PYR, light green, PDB 3QGT) and CYC (TM4-CYC, cyan, PDB 3UM8) shows no significant difference in overall structure and ligands binding in the active-site pocket. (B) The PYR complex of mutant A16V+S108T *Pf*DHFR (T9/94-PYR, pink, PDB id: 3UM5) was superimposed on that of TM4-PYR (light green). The *p*-Cl group of PYR (green sphere) in TM4 has only a minor steric conflict with the γ-CH_3 group of T108 of T9/94 (pink sphere). Hence, PYR in T9/94 is slightly shifted (0.8 Å), and its ring twisting was observed. (C) T9/94-CYC (light orange, PDB 3UM6) was superimposed on TM4-CYC (cyan). A slight shift of enzyme backbone and CYC displacement/ring twisting were observed due to steric clashes at the *p*-Cl group of CYC with the γ-CH_3 group of T108 of T9/94 and one of the two methyl groups of CYC with the γ-CH_3 group of V16 of T9/94, as indicated by spheres. (D) Superposition of T9/94-PYR (pink) and T9/94-CYC (light orange) shows displacement and ring twisting of CYC compared to PYR. The side chains of residues within 3.5 Å around the ligands are shown and labeled. Oxygen, nitrogen, sulfur, and chlorine atoms are colored red, blue, yellow, and green, respectively.

a bacterial complementation assay in the presence of trimethoprim to inhibit host DHFR (Table 2). These A16X active mutants were confined to those amino acids with small aliphatic side chains, likely due to restriction in space around the substrate binding area for this residue. However, residues with either charged (D and E) or γ/δ-polar side chains (Q and N) also cannot replace A at position 16, indicating that factors other than space around this area are also important.

Among the A16X mutants, A16C and A16C+S108T mutants exhibited the highest catalytic efficiency (k_{cat}/K_m) and enzyme turnover rate (k_{cat}). These mutants have not been found in nature, probably due to the fact that the A16C mutation requires changes of all three codon nucleotides (from GCA to UGU/C). Unlike A16C mutants, the A16S and A16G mutants have been found in nature. Despite poor catalytic properties and high PYR sensitivity of the A16G mutant, *P. falciparum* harboring A16G mutant, Santa Lucia strain, was isolated from El Salvador and adapted in monkeys for vaccine development (5, 6). The A16S mutant, on the contrary, showed resistance to all of the antifolates tested, including PYR. Parasites harboring the A16S mutant could survive under low PYR pressure *in vitro* (22). In addition, the A16S+C59R mutant parasite has also been identified in Pakistan under Fansidar (PYR–sulfadoxine) pressure without any mutation in the dihydropteroate synthase gene (25). Based on the *Pf*DHFR-TS structure, C59R appears to play a rescuing role on enzyme activity, enhancing substrate binding through ionic attraction with the glutamate moiety (28). The identification of A16S+C59R thus confirms the PYR-resistant phenotype of A16S and supports our finding of antifolate resistance (CYC and PYR) of this mutant. The A16S+S108T double mutant has better kinetic properties and is more CYC resistant than the A16S single mutant. However, this double mutant is more sensitive to PYR than the A16S mutant (Table 4), explaining why it was not found in the nature under PYR or Fansidar pressure. In the background of S108N mutation, none of the five A16X mutants with small amino acid side chains (G, C, S, T, and V) could give rise to active DHFR enzyme. This finding is in line with previous observations, where further mutations of A16V+S108N yielded protein with no DHFR activity (18). These findings suggest that the areas around A16 and S108 in the active- site cleft are crucial for substrate binding. In short, mutation is limited by the ability of the substrate to bind with the enzyme leading to catalytic activity. Although S108N mutation alone confers only a low level of CYC and PYR resistance and no further mutation at A16X is possible, the parasite adopts additional mutations at other residues in the active site such as residues 51, 59, and 164 instead. This narrow evolutionary path of muta-

tion is determined by the fitness of antifolate-resistant variants (7, 12, 18), which explains why these mutations are commonly found in the field (26).

Compounds C17 and C88 (15, 27) were used to investigate the implications of steric clash from both A16X and S108T/N series. C17, a CYC derivative with one methyl group removed, is expected to avoid the hindrance at position 16. However, except for the naturally occurring A16V+S108T mutant, the K_i values of C17 for most of the selected active mutants are higher than those of CYC, which is probably complicated by the nature of the amino acid at position 16. The polar amino acids at position 16 affect not only the space available for DHF or inhibitor binding but also likely interact with the nicotinamide moiety of NADPH, as revealed by lower NADPH K_m values (Table 3). Presumably, interaction of A16C/S/T with the amino group of the nicotinamide ring shifts the ring toward the DHF or inhibitor site, resulting in decreased affinity for C17 as the site is in part restricted by NADPH. In comparison to C17, C88 with *m*-Cl in place of *p*-Cl has little constraint at position 108, and the K_i values are reduced dramatically in the S108T/N series. C248, which is a desmethyl CYC derivative with an *m*-Cl group, shows K_i values similar to those of C88 for the A16X and most of A16X+S108T mutants, indicating that the inhibitor is more susceptible to the clash at position 108 than at position 16. However, the A16V+S108T mutant is more sensitive to C248 and C17, suggesting that relaxed binding occurs at position 16 irrespective of whether an *m*- or *p*-Cl substituent is present in the vicinity of position 108.

The crystal structure of *Pf*DHFR-TS T9/94 (A16V+S108T) in complex with CYC (T9/94-CYC) confirms that CYC resistance of T9/94 is due to steric conflict of the β-methyl group of A16V and one of 2,2-dimethyl groups of CYC, together with the S108T and *p*-Cl group of CYC (Fig. 1B). For the S108N mutant, there is space restriction imposed on both PYR and CYC due to the amino group of S108N, which could clash with the *p*-Cl groups of both compounds. However, the displacement of PYR from the conflict with S108N is less because the side chain of S108N twists, with a push on NADPH, as observed in the structures of PYR complex of *Pf*DHFR-TS mutants (C59R+S108N and N51I+C59R+S108N+I164L) and S58R+S117N *Pv*DHFR (10, 23, 28). In comparison, the side chain of T108 retains its conformation in complexing with PYR or CYC (Fig. 1A), suggesting space restriction. These mutants, e.g., S108N and A16V+S108T, bind reasonably well with DHF in optimal constraint from both positions as revealed from K_m and K_i (Tables 3 and 4), whereas A16V+S108N, an inactive mutant, may pose steric clash dramatically with DHF. Hence, it can be concluded that S108T has a more direct effect on the *p*-Cl group of CYC than that of PYR, whereas S108N affects the binding of both inhibitors. The double mutation A16V+S108T further reduces active-site space available for CYC, with little effect on PYR, which has no steric conflict around the A16V site. On the other hand, WR99210 binds comfortably with the A16 mutant series mainly due to its flexibility, as reflected by the K_i values (Table 4). The steric clash of a 2-methyl group of CYC with A16V side chain in T9/94-CYC supports our previous hypothesis based on molecular modeling and inhibitors testing (15, 27) and gives a more exact explanation of the difference in sensitivity to CYC and PYR.

In a recent modeling study (13), it was predicted that the S108T mutant has increased stability by van der Waals interactions with neighboring residues and greater affinity for NADPH than does the S108N mutant. This prediction is generally supported by our X-ray structural data. Our report further explains why A16V+S108T is the sole member of the S108T series identified from CYC-resistant parasites since 1977 (6, 24). The blind alley for this series is due to its susceptibility to PYR and limitation of further mutation imposed by necessity for residual enzyme activity. The limitation of DHFR mutations described here offers hope for drug development against resistant parasites, highlighting the potential of focusing on the parts of the target where resistant mutation is constrained by its biological activity, which is essential for the survival of the parasite.

ACKNOWLEDGMENTS

This research was supported by grants from the Wellcome Trust and the MMV Programme, WHO/TDR, Synchrotron Light Research Institute (Public Organization), Thailand, Thailand TDR Programme and NSTDA Cluster and Program Management Office to the team. S.K. is an international scholar of Howard Hughes Medical Institute.

We thank Philip Shaw for manuscript editing.

REFERENCES

1. **Brünger AT, et al.** 1998. Crystallography and NMR system: a new software suite for macromolecular structure determination. Acta Crystallogr. D Biol. Crystallogr. **54**:905–921.
2. **Chitnumsub P, et al.** 2004. Characterization, crystallization and preliminary X-ray analysis of bifunctional dihydrofolate reductase-thymidylate synthase from *Plasmodium falciparum*. Acta Crystallogr. D Biol. Crystallogr. **60**:780–783.
3. **Chothia C.** 1976. The nature of the accessible and buried surfaces in proteins. J. Mol. Biol. **105**:1–12.
4. **Chusacultanachai S, Thiensathit P, Tarnchompoo B, Sirawaraporn W, Yuthavong Y.** 2002. Novel antifolate resistant mutations of *Plasmodium falciparum* dihydrofolate reductase selected in *Escherichia coli*. Mol. Biochem. Parasitol. **120**:61–72.
5. **Collins WE, Galland GG, Sullivan JS, Morris CL, Richardson BB.** 1996. The Santa Lucia strain of *Plasmodium falciparum* as a model for vaccine studies. II. Development of *Aotus vociferans* as a model for testing transmission-blocking vaccines. Am. J. Trop. Med. Hyg. **54**:380–385.
6. **Collins WE, Warren M, Skinner JC, Chin W, Richardson BB.** 1977. Studies on the Santa Lucia (El Salvador) strain of *Plasmodium falciparum* in *Aotus trivirgatus* monkeys. J. Parasitol. **63**:52–56.
7. **Costanzo MS, Brown KM, Hartl DL.** 2011. Fitness trade-offs in the evolution of dihydrofolate reductase and drug resistance in *Plasmodium falciparum*. PLoS One **6**:e19636. doi:10.1371/journal.pone.0019636.
8. **Jones TA, Zou JY, Cowan SW, Kjeldgaard M.** 1991. Improved methods for building protein models in electron density maps and the location of errors in these models. Acta Crystallogr. A **47**(Pt 2):110–119.
9. **Kamchonwongpaisan S, Vanichtanankul J, Taweechai S, Chitnumsub P, Yuthavong Y.** 2007. The role of tryptophan-48 in catalysis and binding of inhibitors of *Plasmodium falciparum* dihydrofolate reductase. Int. J. Parasitol. **37**:787–793.
10. **Kongsaeree P, et al.** 2005. Crystal structure of dihydrofolate reductase from *Plasmodium vivax*: pyrimethamine displacement linked with mutation-induced resistance. Proc. Natl. Acad. Sci. U. S. A. **102**:13046–13051.
11. **Laskowski RA, MacArthur MW, Moss DS, Thornton JM.** 1993. PROCHECK: a program to check the stereochemical quality of protein structures. J. Appl. Crystallogr. **26**:283–291.
12. **Lozovsky ER, et al.** 2009. Stepwise acquisition of pyrimethamine resistance in the malaria parasite. Proc. Natl. Acad. Sci. U. S. A. **106**:12025–12030.
13. **Mharakurwa S, et al.** 2011. Malaria antifolate resistance with contrasting *Plasmodium falciparum* dihydrofolate reductase (DHFR) polymorphisms in humans and *Anopheles* mosquitoes. Proc. Natl. Acad. Sci. U. S. A. **108**:18796–18801.
14. **Otwinowski Z, Minor W.** 1997. Processing of X-ray diffraction data collected in oscillation mode. Methods Enzymol. **276**:307–326.

15. **Rastelli G, et al.** 2000. Interaction of pyrimethamine, cycloguanil, WR99210 and their analogues with *Plasmodium falciparum* dihydrofolate reductase: structural basis of antifolate resistance. Bioorg. Med. Chem. **8**:1117–1128.
16. **Schrödinger LLC.** 2010. The PyMOL molecular graphics system, version 1.3r1. Schrödinger, Rockville, MD.
17. **Sirawaraporn W, Prapunwattana P, Sirawaraporn R, Yuthavong Y, Santi DV.** 1993. The dihydrofolate reductase domain of *Plasmodium falciparum* thymidylate synthase-dihydrofolate reductase. Gene synthesis, expression, and anti-folate-resistant mutants. J. Biol. Chem. **268**:21637–21644.
18. **Sirawaraporn W, Sathitkul T, Sirawaraporn R, Yuthavong Y, Santi DV.** 1997. Antifolate-resistant mutants of *Plasmodium falciparum* dihydrofolate reductase. Proc. Natl. Acad. Sci. U. S. A. **94**:1124–1129.
19. **Sirawaraporn W, et al.** 2002. Mutational analysis of *Plasmodium falciparum* dihydrofolate reductase: the role of aspartate 54 and phenylalanine 223 on catalytic activity and antifolate binding. Mol. Biochem. Parasitol. **121**:185–193.
20. **Tanaka M, Gu HM, Bzik DJ, Li WB, Inselburg J.** 1990. Mutant dihydrofolate reductase-thymidylate synthase genes in pyrimethamine-resistant *Plasmodium falciparum* with polymorphic chromosome duplications. Mol. Biochem. Parasitol. **42**:83–91.
21. **Tarnchompoo B, et al.** 2002. Development of 2,4-diaminopyrimidines as antimalarials based on inhibition of the S108N and C59R+S108N mutants of dihydrofolate reductase from pyrimethamine-resistant *Plasmodium falciparum*. J. Med. Chem. **45**:1244–1252.
22. **Thaithong S, et al.** 2001. *Plasmodium falciparum*: gene mutations and amplification of dihydrofolate reductase genes in parasites grown *in vitro* in presence of pyrimethamine. Exp. Parasitol. **98**:59–70.
23. **Vanichtanankul J, et al.** 2011. Trypanosomal dihydrofolate reductase reveals natural antifolate resistance. ACS Chem. Biol. **6**:905–911.
24. **Volkman SK, et al.** 2007. A genome-wide map of diversity in *Plasmodium falciparum*. Nat. Genet. **39**:113–119.
25. **Wang P, et al.** 1997. Resistance to antifolates in *Plasmodium falciparum* monitored by sequence analysis of dihydropteroate synthetase and dihydrofolate reductase alleles in a large number of field samples of diverse origins. Mol. Biochem. Parasitol. **89**:161–177.
26. **Yuthavong Y.** 2002. Basis for antifolate action and resistance in malaria. Microbes Infect. **4**:175–182.
27. **Yuthavong Y, et al.** 2000. Development of a lead inhibitor for the A16V+S108T mutant of dihydrofolate reductase from the cycloguanil-resistant strain (T9/94) of *Plasmodium falciparum*. J. Med. Chem. **43**:2738–2744.
28. **Yuvaniyama J, et al.** 2003. Insights into antifolate resistance from malarial DHFR-TS structures. Nat. Struct. Biol. **10**:357–365.
29. **Zamyatnin AA.** 1972. Protein volume in solution. Prog. Biophys. Mol. Biol. **24**:107–123.